ACS Sustainable Chemistry and Engineering, Volume 9, Issue 20, pp. 7063-7073
DOI:10.1021/acssuschemeng.1c01048

Dynamic transformations of metals in the burning solid matter during combustion of heavy metal-contaminated biomass

Jianrui Zha [†], *Yaji Huang** [†], *Zhicheng Zhu* [†], *Mengzhu Yu* [†], *Peter T. Clough* [‡], *Yongliang Yan* [‡], *Lu Dong* [†], *Haoqiang Cheng* [†]

[†] Key Laboratory of Energy Thermal Conversion and Control of Ministry of Education, School of Energy and Environment, Southeast University, No. 2 Sipailou, Nanjing 210096, China

[‡] Energy and Power Theme, Cranfield University, College Road, Bedford MK43 0AL, United Kingdom

*Corresponding Author. Email: heyyj@seu.edu.cn

ABSTRACT

Combustion as an efficient and reliable method is widely used for metal-enriched biomass to achieve energy and metal recoveries, but there are emission risks of heavy metals in the flue gas and bottom ash that can arise secondary pollutions. To optimise such combustion processes, this work investigated the combustion characteristics of a kind of hyper-accumulator biomass and focused on the intermediate states and dynamic transformations of metals for the first time. A pseudo-*in-situ* sampling method was used to collect the burning solid residues at different time intervals before further analysis. The conversions between elemental forms were revealed, and their changing rates were also calculated. It was found that the transformation of metal was determined by their elemental natures, species distributions and the combustion progress where there was not a consecutive process but separated by several stages, which were related to 1) the release of volatile matters 2) formation and consumption of the char and 3) the fixation by silicates. Based on the information of dynamic metal characteristics, a new strategy was proposed to optimise metal distribution by adjusting combustion time of operations. The methodology introduced in this work will also help emission control and metal recovery for other metal-rich fuels.

KEYWORDS

Hyper-accumulator biomass; Combustion; Heavy metal; Species transformation; Dynamic behaviour.

1. Introduction

Soil contamination by heavy metals has become a serious problem in developing countries, and phytoremediation is regarded as an environmentally-friendly and economical method to remediate this pollution. Phytoremediation is the process whereby some kinds of hyper-accumulator plants are used to absorb elements present in the soil such that heavy metals can be enriched and fixated inside the biomass without extra chemical and energy input [1,2]. However, proper treatment for biomass harvested from these polluted areas is required, because biomass rich in heavy metals can threaten food chains and human health when disposed inappropriately [3–5]. Thermal treatment including combustion, gasification and pyrolysis is an efficient option since the biomass can be reduced into manageable volume [6–9]. Gasification and pyrolysis of such contaminated biomass can produce products such as syngas, oil and char, but these require more complex and immature technologies (tar in the syngas during gasification, inefficiency and lack of commercial application for pyrolysis) and their products inevitably contain heavy metals with difficulty or high price for separation [10,11], so those drawbacks limit the development of these two technologies for treating such contaminated biomass. In comparison, incineration with its high efficiency and reliability became welcomed for this issue which can achieve both energy recovery and metal recovery [12]. However, there are still risks of secondary pollutions during combustion [13–15]. On the one hand, like other typical biomass, many problems are induced by alkali metals such as slagging and particulate matter. Besides, heavy metals can be released within the flue gas through the vaporisation-condensation mechanism and then emitted to the ambient atmosphere. Moreover, high concentrations of heavy metals in fly ash generates new hazardous materials with potential leaching toxicity [13,16,17]. Thus, it is necessary to reveal the behaviours of metals for improving combustion processes and reducing pollutant emissions.

There have been many studies on combustion of those heavy metal enriched biomass, and there are some general conclusions about metal behaviours in a furnace. Temperature is a dominate factor for combustion kinetics and also has a significant effect on transformations of metals [15,18]. A reducing

atmosphere can enhance the conversions of metals to their elemental forms which often have a high volatility, whereas in an oxidising atmosphere metals tend to form their oxide forms with much higher melting points, but sometimes the vaporisations of metals also can be stimulated in an oxygen-rich atmosphere due to more violent combustion [19]. The presence of chlorine increases the release of metals through the formation of metal chlorides with low melting points [20–22], while silicates can fix metals to generate stable species in the ash [23–26].

For most studies covering incineration and heavy metal issues, the solid products are analysed to investigate the transference of metals and the toxicity of heavy metals after the thermal process. Besides the properties of the fuel and the combustion conditions, the behaviour of metals depends on their elemental nature including their melting points and saturated vapour pressures, and is also related to their species in the raw fuel [24,27]. These results only considered the final statuses of the residues, which means the intermediate statuses were unknown for the minor or trace elements in the burning solid fuels. If the process of metals in the solid phase can be clarified, the mechanism of metal transference can be further revealed, and in turn the combustion process can also be improved for fuels with harmful metals [28]. In some previous works, fuels were initially leached by different extraction agents before ignition to remove a certain ‘metal form’, such as a water soluble form or acetic acid soluble form, to determine the behaviours of each metal species during combustion [29–31]. Unfortunately, there were potential conversions between metal forms in the solid phase during the combustion, but this effect seems to be ignored before. Though the metals released in the flue gas can be measured by an inductively coupled plasma optical emission spectroscopy (ICP-OES) in real-time or *in-situ* detected by laser-induced breakdown spectroscopy (LIBS) [31–34], it is still difficult to measure the metal forms in the solid phase directly by conventional devices at the condition of combustion, where the reactions at high temperatures are fast and inconstant, and the concentrations of some minor or trace elements are too low to be detected. However, it is possible to pause the combustion to obtain the

burning samples with a pseudo intermediate state, which can still offer some useful information in the ongoing process.

This study focused on the dynamic behaviours of metals during combustion of a kind of contaminated biomass with high concentrations of heavy metals. A pseudo-*in-situ* sampling method in a furnace was applied for the first time to gain the burning solid samples, which then were leached by two steps to classify different metal forms. Matched with combustion characteristics, the dynamic transformations of metals were measured and further analysed. Through the methodology in this study, the pseudo intermediate state of metals in the burning samples could be traced. Additionally, based on the new information derived from that experiment, a timing strategy was proposed for optimising the combustion process of such hazardous fuels to control the species distributions of metals.

2. Materials and methods

2.1 The compositions of the fuel

The biomass named *Sedum plumbizincicola*, a hyper-accumulating plant [35,36], was harvested from a heavy metal contaminated ground in South China of which the aboveground part was selected and cut into pieces in the length less than 5 mm. The compositions of the biomass are listed in Table S1, where the major elements of inorganic content were calcium, zinc, potassium and silicon. The concentrations of heavy metals were very high, with 19.8 mg/g for Zn, 560 mg/kg for Pb and 174 mg/kg for Cd.

2.2 Combustion experiment

The combustion tests were conducted in a self-made horizontal tube furnace with a diameter of 30 mm and a height of 400 mm where the airflow rate and the combustion temperature were 30 L/h and 900 ℃ respectively. The biomass (dry basis, 0.2 g) was placed into a 10 mL crucible, which was made of corundum instead of quartz to prevent potential slagging on the vessel surface. To feed the fuel and

pick up the residue quickly, an automated-controlled lifter was used with a refractory platform to hold the crucible.

A diagram of the reactor and the procedures are displayed in Figure 1. As the sample would be still either burning or pyrolysing after being removed from the furnace, and in consideration of probable reactions between minerals in the combustion product and gases in the air, the sample was chilled and quenched in an air free environment immediately after sampling to maintain the integrity of the sample. The method firstly involved placing the crucible on the platform and waiting for temperature stability within the reactor. Once the fuel was moved into the centre of furnace, the timing of combustion was started. The combustion sampling times were set to 15, 30, 45, 60, 90, 120, 160, 200, 330, 420 seconds for each trial. When reaching the set combustion time, the platform was lowered, then the top of crucible would be covered immediately to isolate it from the air. Next, the crucible was moved into an ice tank below 0 ℃ to quench the residue and minimise any potential pyrolysis. Those operations took less than 2 seconds. Finally, the sample was weighted and stored after cooling down. For each sampling point, at least five paralleled trials were conducted for further statistical analysis. It should be noted that the rig must be located in a fume hood or cupboard, and the operator must wear a mask with an active carbon filter, in case of the potential inhalation of harmful flue gas.

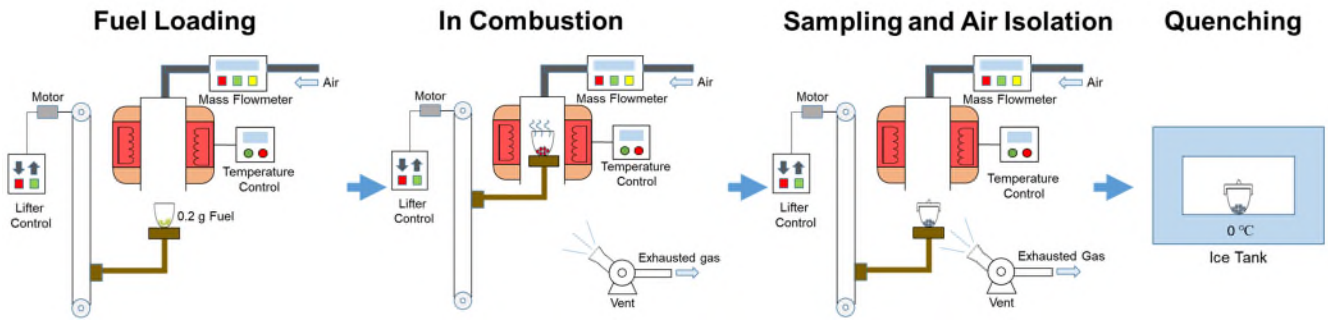

Figure 1 Schematic of combustion test and sampling procedures.

2.3 Analysis methods

The weight loss fraction wl_i and its differential rate v_i during the biomass combustion were calculated as Equation 1 and Equation 2:

$$wl_i = 1 - \frac{W_i}{W_0} \quad (W_0 = 0.2\ \text{g}) \qquad (1)$$

$$v_{i+1/2} = \frac{wl_{i+1} - wl_i}{T_{i+1} - T_i} \qquad (2)$$

Where, the subscript *i* is the serial number of sampling, the subscript *0* means the parameter is derived from initial biomass, W_i is the weight of combustion residue at the number *i* sampling, T_i is the time from the beginning at the number *i* sampling, and the time of *i+1/2* is the midpoint between T_i and T_{i+1}.

Thermogravimetric analysis and differential scanning calorimetry (TGA-DSC, STA-449F3, NETZSCH) was used to resolve the weight loss and heat release peaks under a constant heating rate of 10 ℃/min, and DTG (differential thermo-gravimetric) analysis was calculated based on TGA result. The samples after combustion were digested thoroughly by HCl-HNO_3-HF-$HClO_4$ to obtain the total metal concentrations in the sample. Mass fraction of metal *n* in sample *i* per unit mass of input fuel ($m_{i,n}$) and its metal retention rate ($mr_{i,n}$) were expressed by these following equations:

$$m_{i,n} = \frac{M_{i,n}}{W_0} \qquad (3)$$

$$mr_{i,n} = \frac{M_{i,n}}{M_{0,n}} \qquad (4)$$

Where, $M_{i,n}$ is the total mass of element *n* in the sample *i*.

Additionally, to evaluate the leachability and toxicity of metals, the samples were leached by 20 mL water solution of acetic acid at PH = 3 with stirring for 24 hours to extract metals in their reactive species such as oxides, hydroxides and carbonates. Equation 5 and Equation 6 show the fractions of the leachable-form and the fixed-form of metal *n* per unit mass of input fuel ($l_{i,n}$ and $f_{i,n}$):

$$l_{i,n} = \frac{V \cdot C_{i,n}}{M_{0,n}} \quad (V = 20\ \text{mL}) \qquad (5)$$

$$f_{i,n} = mr_{i,n} - l_{i,n} \quad (6)$$

Where V is the solution volume of acetic acid used in the leaching treatment and $C_{i,n}$ is the concentration of metal n in the leachate solution. To evaluate the characterisations of heavy metal in the ash or char, Equation 7 and 8 present the mass fraction of metal n in the burning solid residue ($ma_{i,n}$) and the estimated leachate concentration ($LC_{i,n}$) which assumed the ash and acid solution were mixed in a solid-liquid proportion of 1:20 (g/mL):

$$ma_{i,n} = \frac{M_{i,n}}{W_i} \quad (7)$$

$$LC_{i,n} = \frac{C_{i,n}}{W_i} \quad (8)$$

The metal concentrations in the solutions from the leaching and digestion were measured by an ICP−OES (Agilent 5110). For those data of weights and metal concentrations, at least three data from the parallel tests were averaged for analysis. Furthermore, the morphologies and crystal phases of the samples were analysed by a scanning electron microscopy with an energy dispersive spectroscopy (SEM−EDS, SU3500, Hitachi) and X-ray diffraction (XRD, D8 Advance, Bruker) respectively.

3. Results and discussion

3.1 Weight loss analysis during combustion

Thermo-gravimetric and heat flux analysis were measured to understand the combustion process of the biomass, of which the results are presented in Figure 2(a). There were three weight loss peaks at 220-380 ℃, 280-510 ℃ and 560-670 ℃. The first and the second peaks represented combustion of volatile matters and fixed carbon respectively, while the third peak did not indicate the combustion reactions but more likely was the decomposition of carbonates, because the biomass contained a large amount of calcium which could absorb CO_2 to form $CaCO_3$ at lower temperatures and then release it at higher temperatures. Another evidence is that there was an endothermic peak as shown in DSC curves. [37]

The mass loss change during the combustion in the horizontal furnace is shown in Figure 2(b), where there were three stages within the whole process. From the start point to 45 seconds, there was a sharp weight loss for the fuel which can be attributed to a rapid ignition of volatile matters, when this stage is named as the quick combustion stage. [38] The second stage between 45-330 seconds was defined as slow combustion stage, where there was steady and slow weight loss. The remaining of the volatile matters and fixed carbon were burned in this period. The peak mass loss rate occurred at ~200 seconds which could be due to the CO_2 release from carbonates. When the mass was constant, the biomass stopped combusting and this period was named the burnout stage.

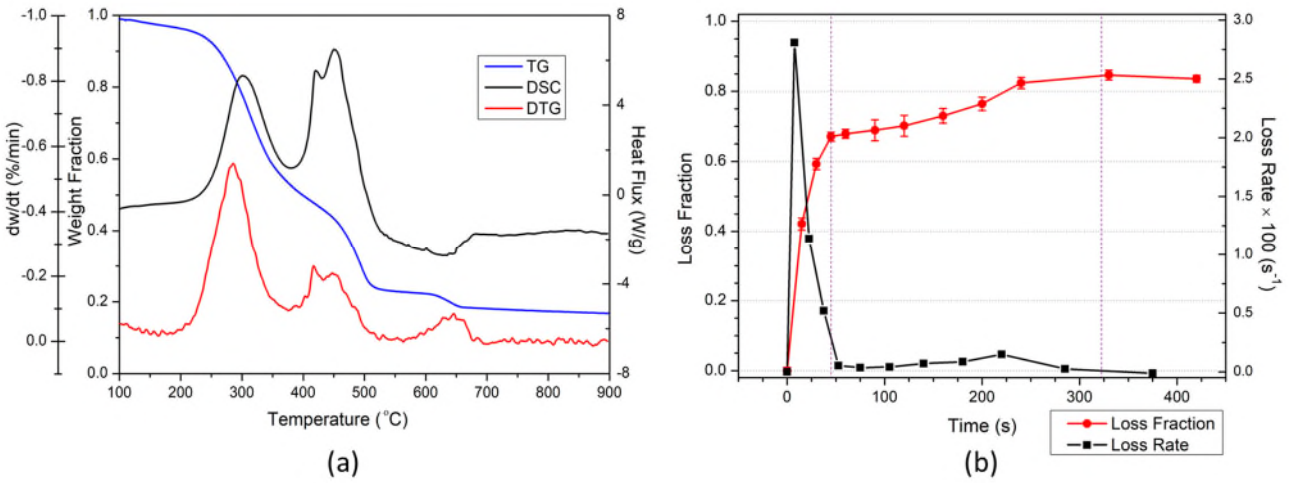

Figure 2 Combustion characteristics of the biomass. (a) TG, DTG and DSC curves of biomass at 10 ℃/min heating rate. (b)Weight loss fraction and weight loss rate at 900 ℃.

3.2 Evolution of main crystal minerals in the residue

The mineral phases were changed during combustion, which can affect both the behaviours of heavy metals and the utilization of ash or char. Detailed XRD analysis curves are shown in Figure S1. Feldspar was the only crystal occurring at 15 seconds, which means other elements were non-crystalline or were free phases at the beginning of ignition. At 30 seconds, quartz, zinc oxide and calcite were crystallised, while potassium crystals were not found, indicating the species of this element was converted from feldspar to amorphous forms. No new crystal was generated until 160

seconds in the slow combustion stage when lime was generated which was the signal of calcite decomposition, and the temperature in the char particle should have reached to a high level. Also, the quick release of CO_2 could further prove the reason for the weight loss rate peak at 200 seconds. Larnite was formed at 200 seconds, which was the product of the reaction between SiO_2 and CaO. Then at 240 seconds, the end of the second stage, kalsilite ($KAlSiO_4$) was formed, the formula of which chemical has fewer silicon oxides than that of feldspar ($KAlSi_3O_8$), Therefore, some of the potassium minerals in the fuel or ash underwent a decomposition process from feldspar to quartz and amorphous potassium (aluminosilicates) to kalsilite. At 330 seconds when the burnout stage started, calcite disappeared, and the formation of hardysonite ($Ca_2ZnSi_2O_7$) indicated that under high temperatures and with a longer time, further eutectic transformation began with high melting point minerals of zinc oxide. Finally, no further changes in crystal species were observed at 420 seconds.

It can be concluded that though there was a quick mass change at the early period of the combustion, the evolution of crystal phases was little changed. But there were more frequent generations of new crystal species and phase disappearances in the latter period of combustion, which can be attributed to the higher temperatures during the char burning. It also should be noted that there could be a considerable proportions of the mineral content not having been detected because they were in amorphous phases [39].

3.3 Morphology of the burning biomass

The morphologies of the biomass and its burning residue presented two kinds of surface, a smooth one and a rough one, indicating the components of the biomass can be classified into two parts, as displayed in Figure 3a-s and 3a-r. It seems that the smooth surface was the fibre of the biomass as its veins were in lines, while the rough surface might be a part of the leaf, where broken surface might be caused by the drying process in the pre-treatment. According to the EDS analysis in Table S2, the smooth surface

contained more carbon and less silicon so that this structure was the dominant component in the stem, while there were various minerals and less organic in the rough surface.

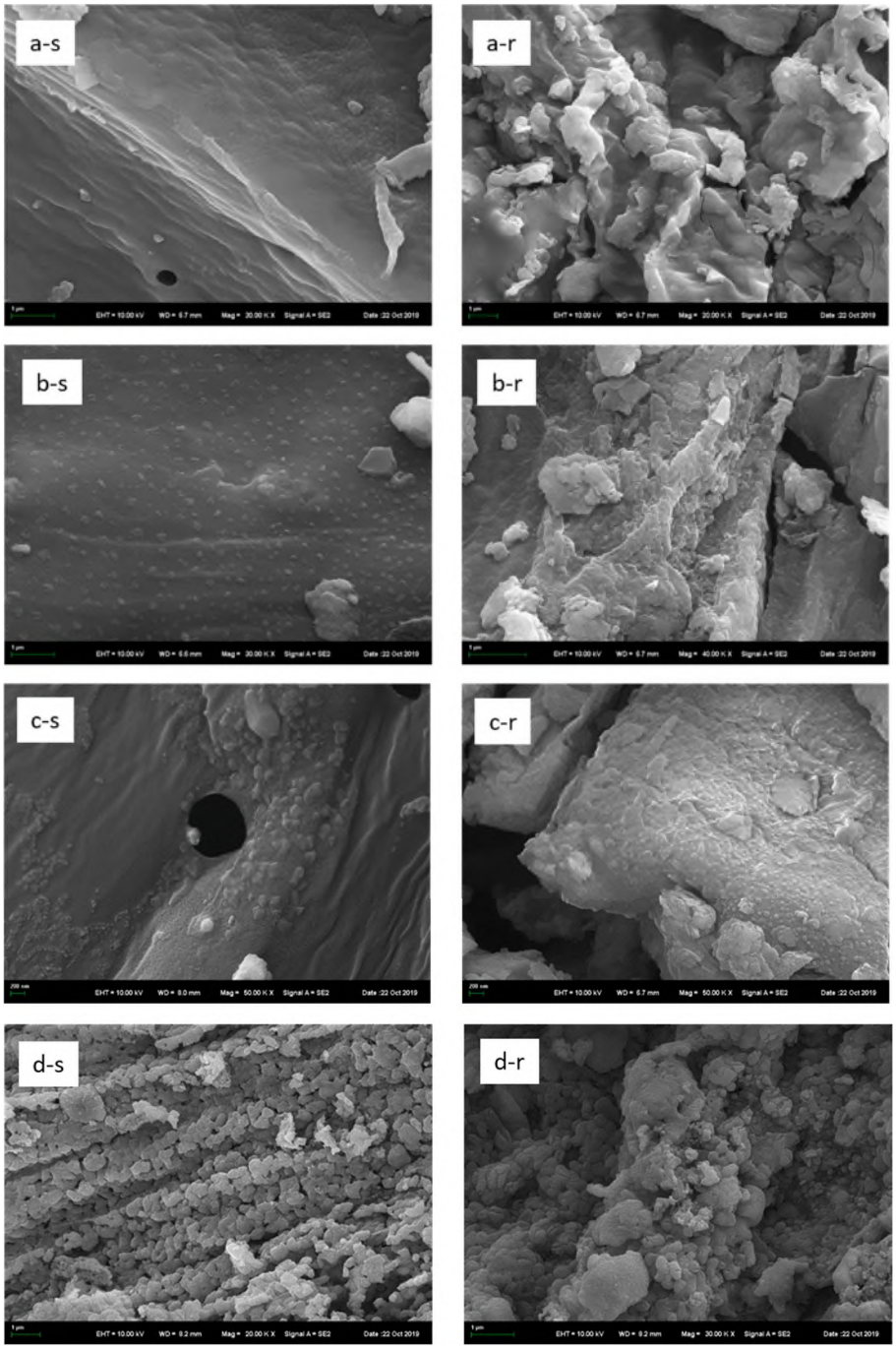

Figure 3 SEM images of the smooth (s) and rough (r) surfaces in the raw biomass and its burning residue. (a) 0 s; (b) 30 s; (c) 200 s; (d) 330 s.

For the smooth part, crystals appeared during the quick combustion stage (Figure 3b-s) and their size grew and looked gradually clear with the char burning (Figure 3c-s). Finally, when the char was burnt,

mineral particles in the homogeneous size of 200-400 nm were laid in arrows (Figure 3d-s). Based on elemental analysis in Table S2, the crystals mainly consisted of calcium oxide.[40] Although the concentration of potassium was at the similar level, this element did not seem to enrich after combustion, so potassium in the smooth part could be transferred to elsewhere or vaporised directly during the thermal process. [41,42]

In the rough surface part, the growth of crystal was more remarkable than that in the smooth part, and the distribution of particles was disordered. Additionally, those particles were agglomerated and melted into bigger ones in and after the second combustion stage (Figure 3c-r and 3d-r), and the carbon surrounded with some of them was burnt out earlier than that in the smooth surface, as listed in EDS analysis. Those phenomena could be attributed to the interactions of mineral compositions including potassium, calcium, zinc, silicon and aluminium, which resulted in eutectic melting and diverse particles. [42,43]

3.4 The dynamic behaviours of metals during combustion

To analyse the behaviours of metals, the samples withdrawn at different stages of the combustion were digested according to section 3.2 and the leachable and residual forms were analysed by ICP-OES; their partition changes were calculated according to Equation 4-6. The mass fractions of calcium, aluminium and iron varied little from their initial values, as they are non-volatile elements at high temperature (absolute values of the metal mass changes are shown in Figure S2 based on Equation 3), thus the retention rates of those three metals were approximately set as one to normalise the form fractions in the solid residue (Figure 4). Other elements are semi-volatile metals and a part of them was released to the gaseous phase during thermal treatment. Considering their different natures, behaviours of the two kinds of metals are discussed respectively.

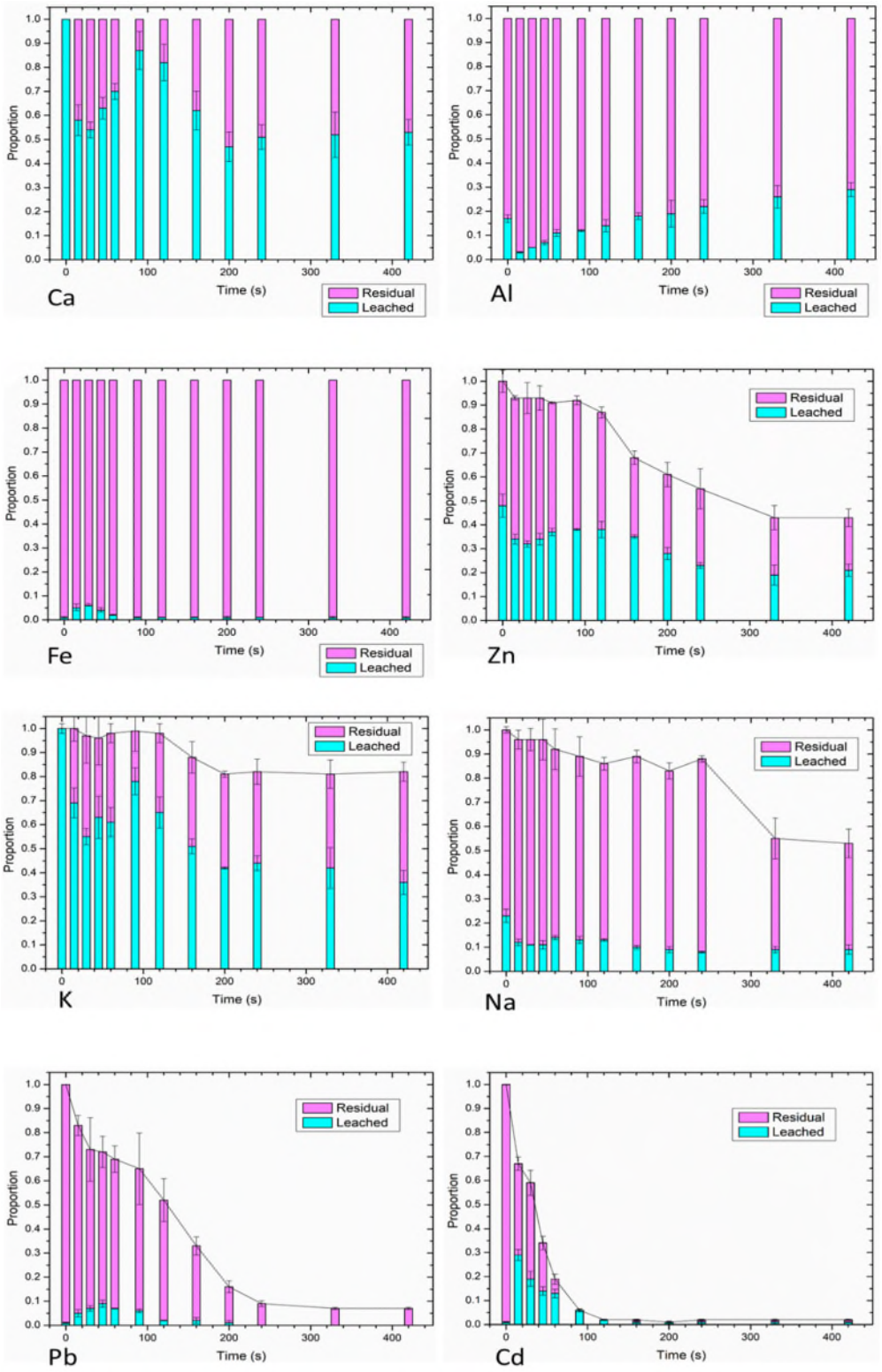

Figure 4. Dynamic distributions of metals during combustion

3.4.1 Non-volatile metals

Calcium: In the raw biomass, the calcium was 100% soluble so that it could be transported easily within the biomass when living. When the biomass was sent into the furnace, over 40% of calcium

was immediately transferred to an insoluble form, and the proportion of residual form decreased until 90 seconds. The decline of the leachability after ignition could be due to the formation of char, which can adsorb metal ions during the leaching step meaning that some of the calcium did not enter the leachate. This explanation can also be proved because with the continual consumption of the char, the adsorption capacity of metal ions decreased when leached, and calcite/lime can be thoroughly dissolved by acetic acid [30]. Then the fixed-form of calcium slightly increased again, which could be as a result of the reaction with silicates and generating more stable minerals such as larnite (see XRD results), and other amorphous calcium silicates which could not be detected by XRD could also have be formed.

Aluminium: About 1/6 of the aluminium was soluble in the raw biomass, while at 15 seconds the value was only 2% and then gradually increased. According to the XRD results, the elemental aluminium was in the form of aluminosilicates, which is often stable in the acid solution. However, its reactivity increased when the stoichiometric number of silicon decreased among the aluminosilicate system. For example, the conversion from feldspar ($KAlSi_3O_8$) to kalsilite ($KAlSiO_4$) caused the aluminium atoms in the aluminosilicate lattice to bond with a smaller proportion of the silicates, which promoted its leachable fraction [39].

Iron: The iron was almost insoluble in the biomass and the burning residue. Its leachable-form of 5% was generated at the beginning of combustion, which might be due to the conversion from organic iron in the biomass to the free form in the char. Then during combustion, all iron converted to the residual form while its leachable-form disappeared.

3.4.2 Semi-volatile metals

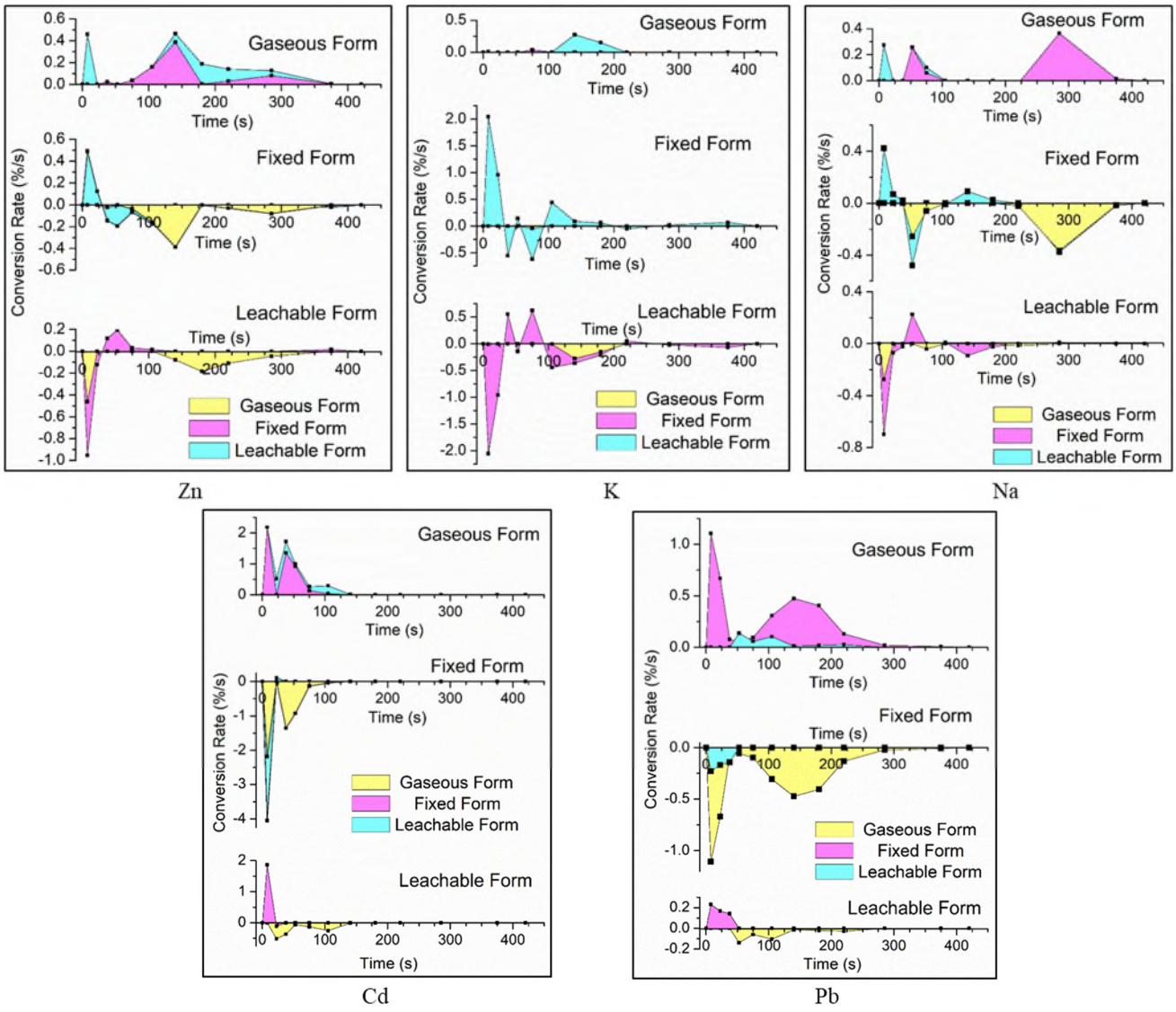

Figure 5. Transformation streams of semi-volatile metals during combustion

The behaviours of semi-volatile metals included both transformation within the solid phase and the solid-to-gas phase, so, there were three potential conversions for an element during the combustion:

A. Fixed-form ⇌ Leachable-form

B. Fixed-form → Gaseous-form

C. Leachable-form → Gaseous-form

While the conversion A is reversible, the conversions B and C are irreversible. Set the conversion rates as v_a (positive direction), v_b, v_c and the generation rates of forms as v_f, v_g and v_l for the fixed-form, gaseous-form and leachable-form respectively. Accordingly, there are

$$v_a + v_b = -v_f \quad (9)$$

$$v_b + v_c = v_g \quad (10)$$

$$-v_a + v_c = v_l \quad (11)$$

Where the net conversion rates of each form (v_f, v_g and v_l) were available, but here we cannot calculate v_a, v_b and v_c directly because $v_f + v_g + v_l = 0$. To simplify the model, we assumed a kind of apparent conversion rates, where each form was either the start or the end of the stream, which means the +/- symbols whether it exported or imported to the stream was determined by the net conversion rate of the form. For example, if the fraction of the fixed-form decreased at some time, it would be regarded as transformed to other species but not converted from the leachable-form, and vice versa. Based on this logic, the apparent conversion rates of metal forms were calculated and displayed in Figure 5.

Zinc: About half of the zinc was stable in the raw biomass. At the beginning of the combustion, there was a release peak of 7% zinc from the leached species which could have resulted from the vaporisation of some soluble organic zinc with low evaporation temperatures, and a conversion peak to fixed-form could be attributed to the formation of char to stabilise the free zinc. Then, a bit of fixed-form returned to leachable-form (maybe its oxide or other inorganic salts) due to the consumption of char at the second combustion stage. During 90-330 seconds, more zinc was vaporised and mostly from its fixed-form, because zinc in fixed-form tended to be reduced by organics to release gaseous zinc so that there was a sharper and shorter releasing peak indicating its stronger reactivity, while the peak of leachable-form was flatter when the inorganic zinc slowly reacted with char and formed atom zinc at a higher temperature as Equation 12 until all the char was burnout and only 3/7 of zinc remained in the ash [16,27,44].

$$MO_{0.5x} + 0.5xC = 0.5xCO(g) + M(g)\ (x \text{ is the metal valence}) \quad (12)$$

Potassium: This element was soluble in the initial fuel, and its behaviours before 90 seconds were similar to that of calcium. Then about 1/6 of potassium was vaporised from its leachable-form because of the higher temperature during char combustion and the reduction effect of char to generate metal

vapour. Since alkali metals tend to form their carbonate during combustion, [45] a possible reaction for metal vaporisation could be:

$$Am_2CO_3 + 2C = 2Am(g) + 3CO(g) \quad (13)$$

where, symbol Am refers to alkali metal (K and Na). This reaction occurred at a higher temperature than the oxides reduction reaction as Equation 13 (see thermal equilibrium calculations in Figure S3). Gradually, its combination with aluminosilicates increased the proportion of its fixed-form at the same time.

Sodium: Below a quarter of sodium was leachable in the raw biomass, from which a part of the metal was vaporised at the first combustion stage, and there was a conversion to the fixed-form. Between 45-60 seconds, there were a release peak and a formation peak of leached species from the fixed-form, and then some of the leachable-form sodium was slowly transformed to its fixed-form until 200 seconds. The first two vaporising peaks revealed the different species of sodium in the biomass, while the three form transformations indicated the formation and consumption of the char and the fixation by silicates. The retention of sodium dramatically declined during 240-330 seconds when the temperature of the char was highest, where the reaction could occur as Equation 13. Since no char remained at the burnout stage, the vaporisation of sodium stopped.

Cadmium: This hazardous element existed as a fixed-form in the biomass. As a high-volatile metal in the furnace, cadmium was rapidly vaporised upon ignition and only 6% remained in the char at 90 seconds. Simultaneously there was the formation of the fixed-form which also released gaseous cadmium. There were two release peaks from the fixed-form before 90 seconds, indicating two species of organic cadmium in the biomass. Then there were almost only leachable-forms remaining in the char, which was slowly vaporised, probably because of the reduction reaction (Equation 12) with the inorganic cadmium by char. Since the middle term of the second combustion stage, some of the leachable-form of cadmium was gradually transformed to the fixed-form due to the combination with silicates, and about 2% remained in the ash eventually [24,39].

Lead: Similar with cadmium, lead also presented as the fixed-form in the raw biomass and had the same number and sequence of transformation peaks, but the curve of lead was smoother where the transformations also raised later than that of cadmium, indicating the lower reactivity of lead. Additionally, its release continued until the burnout stage, when the reduction agent, char, ran out, leaving 6% of the lead in fixed-form remained in the ash which could be stabilised by silicates.

3.5 Dynamic concentration and leachate characteristics of heavy metals in the solid phase

The concentrations of three heavy metals (zinc, lead and cadmium) in the solid matters (biomass, char and ash) and its leachate are listed in Table 1 (calculated by Equation 7 and 8), where the values of leaching characteristics in the residue can reflect its toxicity to the environment.

The change of metal concentrations in the solid depended on both rates of combustion and metal release. The concentrations of all the three metals increased rapidly in the early combustion period because of the high ratio of weight loss through devolatilisation. Then the concentrations of lead and cadmium decreased because the rate of weight loss through char combustion was much slower than the vaporisations of the two metals, while the trend of zinc was almost flat due to its slower release rate. The highest concentrations and their sampling times for heavy metals were 58 mg/g at 120 seconds for zinc, 353 μg/g at 60 seconds for lead and 711 μg/g at 30 seconds for cadmium.

The leached fractions of zinc in the solid phase increased and then floated over 40% after 60 seconds. As zinc concentration in the leachate was very high, plenty of the metal in the solid phase can be easily extracted and recovered as a form of metal mining, while on the other hand it made the ash or char harmful when considering leachate toxicity. For lead, its concentrations in the ash leachate were extremely low after 240 seconds, which contributed little to leachate toxicity, because lead in the solid phase could be fixed by silicates after a longer thermal treatment. Cadmium had a much higher leachability than lead, of which even 95.2% in the char could be extracted at 90 seconds. The

concentration of cadmium in the leachate also has the lowest value at 240 seconds because the remained char could help to adsorb the metal in the aqueous solution.

Table 1 Concentrations of heavy metals (Zn, Pb, Cd) and their leachable fraction in the solid matter

Time /s	Concentrations in the solid			Concentrations in the leachate (1 g: 20 mL)			Leached fractions in the solid (%)		
	Zn (mg/g)	Pb (μg/g)	Cd (μg/g)	Zn (g/L)	Pb (mg/L)	Cd (mg/L)	Zn	Pb	Cd
0	19	171	549	0.47	0.11	0.26	49.5	1.3	0.9
15	31	245	635	0.57	0.70	13.64	36.8	5.7	43.0
30	39	273	711	0.68	1.36	11.64	34.9	10.0	32.7
45	47	322	483	0.86	2.09	10.03	36.6	13.0	41.5
60	52	353	308	1.07	1.86	10.69	41.2	10.5	69.4
90	53	332	95	1.10	1.43	4.52	41.5	8.6	95.2
120	58	307	40	1.28	0.71	1.48	44.1	4.6	74.0
160	51	214	32	1.31	0.62	1.00	51.4	5.8	62.5
200	52	117	29	1.18	0.41	0.90	45.4	7.0	62.1
240	57	85	44	1.21	0.01	0.87	42.5	0.2	39.5
330	56	84	56	1.24	0.01	1.61	44.3	0.2	57.5
420	56	77	56	1.35	0.01	1.50	48.2	0.3	53.6

3.6 Discussion

3.6.1 Behaviours of semi-volatile metals

Since the non-volatile metals (calcium, iron and aluminium) in this plant are harmless to the environment, here we discuss the behaviours of semi-volatile metals which have potential or directly harm. In Figure 5, it seems that the behaviours of zinc, potassium and sodium had similarities while cadmium and lead can be included in another group.

For zinc, potassium and sodium, there were: (1st combustion stage) slight volatilisations of organic metals with low vaporisation points (except potassium) and conversions with high rates to the fixed-form from the leachable-form due to the formation of char that can stabilise elements; (2nd combustion stage) conversions to the leachable-form because of the consumption of the char and oxidation, then the char reduced metals to be dramatically vaporised, where evidence was that the second main peak

was contributed from the metal combined with the char (fixed-form); (from about 90s to the 3rd combustion stage) slowly conversions to fixed-form probably because of stabilised by silicates. Additionally, the conversion rates between fixed-form and leachable-form approximately depended on the fraction of the leachable-form when considering the distribution values in Figure 4.

For cadmium and lead, initially, they were both fixed-form and rapidly released at the first combustion stage, which could be the organic metals with low boiling points. Then the second release peak was the reduced elemental form of the metals. According to the thermal equilibrium calculations in Figure S3, the reduction reaction of cadmium starts at a much lower temperature than lead, which explains its higher reactivity.

Though metals performed differently resulted from their natures and initial species, it can be still concluded that the transformation of a metal during combustion was not a consecutive process but separated by several stages, which were related to the release of volatile matters, formation and consumption of the char and the fixation by silicates.

3.6.2 Potential application based on the dynamic behaviours of metals

As the transformations of metals were traced during combustion, we can use this information for incineration furnace design or condition adjustment to reach various purposes of emission control and metal recovery, because both ash deposition and gaseous pollutants emission should be especially considered for fuels with high concentrations of heavy metals. For example, if we hope to maximise the metal collection in the flue gas and the energy recovery, and also minimise the toxicity of the bottom ash, the best time to terminate the combustion is not at the burnout stage, but within the char combustion stage (between 200-240s) when the release of semi-volatile metals is almost completed and a little amount of char remains which helps the stability of metals. When the purposes are both volume reduction and decreasing the total amount of metal vaporisation to control particulate matter emission and ash slagging, 100-120 seconds after ignition would be preferable for the termination at the conditions used in this work.

In a further study, more sequential extraction steps for measuring metal species and a higher frequency of sampling can be conducted to extend the real-time information of metal transformation during combustion. Moreover, other solid fuels can also be tested through this methodology when studying the pathways of metals. Potentially, besides the traditional optimisation methods by adjusting the combustion condition and co-combustion for metal issues [24,26], the new knowledge of metal dynamic behaviours can also help to design the timing of reactions and operations during the thermal treatment of hazardous fuels with heavy metals, including hyper-accumulator biomass, electric waste and industrial sludge, so as to achieve: emissions control, volume reduction or metal recovery.

4. Conclusion

In this work, the combustion characteristics of a hyper-accumulator biomass was studied, where the dynamic behaviours of metals were particularly investigated through in-situ sampling method that was first reported. Three combustion stages were observed where the morphologies and mineral evolutions were detected. Through an approximately *in-situ* sampling method, the metal species in the burning solid matter could be reserved and were extracted by leaching steps. It was found that the transformation rates and times varied from elements. Generally, devolatilisation, the formation and consumption of the char and the fixation of the silicates had direct impact on the transference processes of metals. Moreover, dynamic concentration and leachate characteristics of heavy metals in the solid phase were measured to evaluate the toxicity change of the solid residues during combustion.

The transformations of metals in the solid phase during the combustion were firstly revealed, where the dynamic conversions of different metal forms were traced, including the vaporisation and the leaching characteristics of metals, which may help to design new strategies for heavy metal control and metal mining.

ASSOCIATED CONTENT

Supporting Information

The following files are available free of charge: (1) Composition analysis of the biomass; (2) XRD analysis of the solid matters during combustion; (3) EDS analysis of the raw biomass and its burning residues; (4) Mass changes of metals during combustion; (5) Thermal equilibrium calculations for the reduction reactions by char.

NOTE

The authors declare no competing financial interest.

ACKNOWLEDGMENT

The authors would like to thank for the financial support by National Natural Science Foundation of China (No. 51976036), Key Technologies Research and Development Program (China, No. YFC1901200) and Scientific Research Foundation of Graduate School of Southeast University (No. 3203009748).

Reference

(1) Mahar, A.; Wang, P.; Ali, A.; Awasthi, M. K.; Lahori, A. H.; Wang, Q.; Li, R.; Zhang, Z. Challenges and Opportunities in the Phytoremediation of Heavy Metals Contaminated Soils: A Review. *Ecotoxicol. Environ. Saf.* **2016**, *126*, 111–121. https://doi.org/10.1016/j.ecoenv.2015.12.023.

(2) Kovacs, H.; Szemmelveisz, K. Disposal Options for Polluted Plants Grown on Heavy Metal Contaminated Brownfield Lands – A Review. *Chemosphere* **2017**, *166*, 8–20. https://doi.org/10.1016/j.chemosphere.2016.09.076.

(3) Chalot, M.; Blaudez, D.; Rogaume, Y.; Provent, A. S.; Pascual, C. Fate of Trace Elements during the Combustion of Phytoremediation Wood. *Environ. Sci. Technol.* **2012**, *46* (24), 13361–13369. https://doi.org/10.1021/es3017478.

(4) Grzegórska, A.; Rybarczyk, P.; Rogala, A.; Zabrocki, D. Phytoremediation-from Environment Cleaning to Energy Generation-Current Status and Future Perspectives. *Energies*. 2020. https://doi.org/10.3390/en13112905.

(5) Bernal, M. P.; Gómez, X.; Chang, R.; Arco-Lázaro, E.; Clemente, R. Strategies for the Use of Plant

Biomass Obtained in the Phytostabilisation of Trace-Element-Contaminated Soils. *Biomass and Bioenergy* **2019**, *126*, 220–230. https://doi.org/10.1016/j.biombioe.2019.05.017.

(6) Nzihou, A.; Stanmore, B. The Fate of Heavy Metals during Combustion and Gasification of Contaminated Biomass-A Brief Review. *J. Hazard. Mater.* **2013**, *256–257*, 56–66. https://doi.org/10.1016/j.jhazmat.2013.02.050.

(7) Yang, J. guang. Heavy Metal Removal and Crude Bio-Oil Upgrading from Sedum Plumbizincicola Harvest Using Hydrothermal Upgrading Process. *Bioresour. Technol.* **2010**, *101* (19), 7653–7657. https://doi.org/10.1016/j.biortech.2010.04.095.

(8) Stals, M.; Carleer, R.; Reggers, G.; Schreurs, S.; Yperman, J. Flash Pyrolysis of Heavy Metal Contaminated Hardwoods from Phytoremediation: Characterisation of Biomass, Pyrolysis Oil and Char/Ash Fraction. *J. Anal. Appl. Pyrolysis* **2010**, *89* (1), 22–29. https://doi.org/10.1016/j.jaap.2010.05.001.

(9) Vervaeke, P.; Tack, F. M. G.; Navez, F.; Martin, J.; Verloo, M. G.; Lust, N. Fate of Heavy Metals during Fixed Bed Downdraft Gasification of Willow Wood Harvested from Contaminated Sites. *Biomass and Bioenergy* **2006**, *30* (1), 58–65. https://doi.org/10.1016/j.biombioe.2005.07.001.

(10) Dastyar, W.; Raheem, A.; He, J.; Zhao, M. Biofuel Production Using Thermochemical Conversion of Heavy Metal-Contaminated Biomass (HMCB) Harvested from Phytoextraction Process. *Chem. Eng. J.* **2019**, *358* (August 2018), 759–785. https://doi.org/10.1016/j.cej.2018.08.111.

(11) Šyc, M.; Pohořelý, M.; Jeremiáš, M.; Vosecký, M.; Kameníková, P.; Skoblia, S.; Svoboda, K.; Punčochář, M. Behavior of Heavy Metals in Steam Fluidized Bed Gasification of Contaminated Biomass. *Energy and Fuels* **2011**, *25* (5), 2284–2291. https://doi.org/10.1021/ef1016686.

(12) Sheoran, V.; Sheoran, A. S.; Poonia, P. Phytomining: A Review. *Miner. Eng.* **2009**, *22* (12), 1007–1019. https://doi.org/10.1016/j.mineng.2009.04.001.

(13) Delplanque, M.; Collet, S.; Del Gratta, F.; Schnuriger, B.; Gaucher, R.; Robinson, B.; Bert, V. Combustion of Salix Used for Phytoextraction: The Fate of Metals and Viability of the Processes. *Biomass and Bioenergy* **2013**, *49*, 160–170. https://doi.org/10.1016/j.biombioe.2012.12.026.

(14) Hunce, S. Y.; Clemente, R.; Bernal, M. P. Energy Production Potential of Phytoremediation Plant Biomass: Helianthus Annuus and Silybum Marianum. *Ind. Crops Prod.* **2019**, *135* (January), 206–216.

https://doi.org/10.1016/j.indcrop.2019.04.029.

(15) Yan, X. L.; Chen, T. Bin; Liao, X. Y.; Huang, Z. C.; Pan, J. R.; Hu, T. D.; Nie, C. J.; Xie, H. Arsenic Transformation and Volatilization during Incineration of the Hyperaccumulator Pteris Vittata L. *Environ. Sci. Technol.* **2008**, *42* (5), 1479–1484. https://doi.org/10.1021/es0717459.

(16) Zhong, D. X.; Zhong, Z. P.; Wu, L. H.; Xue, H.; Song, Z. W.; Luo, Y. M. Thermal Characteristics and Fate of Heavy Metals during Thermal Treatment of Sedum Plumbizincicola, a Zinc and Cadmium Hyperaccumulator. *Fuel Process. Technol.* **2015**, *131*, 125–132. https://doi.org/10.1016/j.fuproc.2014.11.022.

(17) Kovacs, H.; Szemmelveisz, K.; Koós, T. Theoretical and Experimental Metals Flow Calculations during Biomass Combustion. *Fuel* **2016**, *185*, 524–531. https://doi.org/10.1016/j.fuel.2016.08.007.

(18) Tarik, M.; Ludwig, C. Evaporation of Metals during the Thermal Treatment of Oxide Nanomaterials in Cellulose-Based Matrices. *Environ. Sci. Technol.* **2020**, *54* (7), 4504–4514. https://doi.org/10.1021/acs.est.9b06359.

(19) Bartoňová, L.; Raclavská, H.; Čech, B.; Kucbel, M. Behavior of Pb during Coal Combustion: An Overview. *Sustain.* **2019**, *11* (21). https://doi.org/10.3390/su11216061.

(20) Lu, P.; Huang, Q.; Bourtsalas, A. C. (Thanos.; Themelis, N. J.; Chi, Y.; Yan, J. Review on Fate of Chlorine during Thermal Processing of Solid Wastes. *J. Environ. Sci. (China)* **2019**, *78*, 13–28. https://doi.org/10.1016/j.jes.2018.09.003.

(21) Wang, X.; Huang, Y.; Liu, C.; Zhang, S.; Wang, Y.; Piao, G. Dynamic Volatilization Behavior of Pb and Cd during Fixed Bed Waste Incineration: Effect of Chlorine and Calcium Oxide. *Fuel* **2017**, *192*, 1–9. https://doi.org/10.1016/j.fuel.2016.12.002.

(22) Xie, K.; Hu, H.; Xu, S.; Chen, T.; Huang, Y.; Yang, Y.; Yang, F.; Yao, H. Fate of Heavy Metals during Molten Salts Thermal Treatment of Municipal Solid Waste Incineration Fly Ashes. *Waste Manag.* **2020**. https://doi.org/10.1016/j.wasman.2019.12.047.

(23) Zha, J.; Huang, Y.; Clough, P. T.; Xia, Z.; Zhu, Z.; Fan, C.; Yu, M.; Yan, Y.; Cheng, H. Green Production of a Novel Sorbent from Kaolin for Capturing Gaseous PbCl2 in a Furnace. *J. Hazard. Mater.* **2021**, *404*, 124045. https://doi.org/10.1016/j.jhazmat.2020.124045.

(24) Zhu, Z.; Huang, Y.; Zha, J.; Yu, M.; Liu, X.; Li, H.; Zhu, X. Emission and Retention of Cadmium during

the Combustion of Contaminated Biomass with Mineral Additives. *Energy and Fuels* **2019**, *33* (12), 12508–12517. https://doi.org/10.1021/acs.energyfuels.9b03266.

(25) Zha, J.; Huang, Y.; Clough, P. T.; Dong, L.; Xu, L.; Liu, L.; Zhu, Z.; Yu, M. Desulfurization Using Limestone during Sludge Incineration in a Fluidized Bed Furnace: Increased Risk of Particulate Matter and Heavy Metal Emissions. *Fuel* **2020**, *273*, 117614. https://doi.org/10.1016/j.fuel.2020.117614.

(26) Yao, H.; Naruse, I. Using Sorbents to Control Heavy Metals and Particulate Matter Emission during Solid Fuel Combustion. *Particuology* **2009**, *7* (6), 477–482. https://doi.org/10.1016/j.partic.2009.06.004.

(27) Zhang, Y.; Chen, Z.; Xu, W.; Liao, Q.; Zhang, H.; Hao, S.; Chen, S. Pyrolysis of Various Phytoremediation Residues for Biochars: Chemical Forms and Environmental Risk of Cd in Biochar. *Bioresour. Technol.* **2020**, *299* (December 2019), 122581. https://doi.org/10.1016/j.biortech.2019.122581.

(28) Li, R.; Chen, Q.; Zhang, H. Detailed Investigation on Sodium (Na) Species Release and Transformation Mechanism during Pyrolysis and Char Gasification of High-Na Zhundong Coal. *Energy and Fuels* **2017**, *31* (6), 5902–5912. https://doi.org/10.1021/acs.energyfuels.7b00410.

(29) Zhang, Y.; Xie, X.; Zhao, J.; Wei, X. The Alkali Metal Occurrence Characteristics and Its Release and Conversion during Wheat Straw Pyrolysis. *Renew. Energy* **2020**, *151*, 255–262. https://doi.org/10.1016/j.renene.2019.11.013.

(30) Jiang, Y.; Ameh, A.; Lei, M.; Duan, L.; Longhurst, P. Solid–Gaseous Phase Transformation of Elemental Contaminants during the Gasification of Biomass. *Sci. Total Environ.* **2016**, *563–564*, 724–730. https://doi.org/10.1016/j.scitotenv.2015.11.017.

(31) Liu, Y.; He, Y.; Wang, Z.; Xia, J.; Wan, K.; Whiddon, R.; Cen, K. Characteristics of Alkali Species Release from a Burning Coal/Biomass Blend. *Appl. Energy* **2018**, *215* (January), 523–531. https://doi.org/10.1016/j.apenergy.2018.02.015.

(32) Huang, Y.; Liu, H.; Yuan, H.; Zhuang, X.; Yuan, S.; Yin, X.; Wu, C. Release and Transformation Pathways of Various K Species during Thermal Conversion of Agricultural Straw. Part 1: Devolatilization Stage. *Energy and Fuels* **2018**, *32* (9), 9605–9613. https://doi.org/10.1021/acs.energyfuels.8b02191.

(33) He, Y.; Qiu, K.; Whiddon, R.; Wang, Z.; Zhu, Y.; Liu, Y.; Li, Z.; Cen, K. Release Characteristic of

Different Classes of Sodium during Combustion of Zhun-Dong Coal Investigated by Laser-Induced Breakdown Spectroscopy. *Sci. Bull.* **2015**, *60* (22), 1927–1934. https://doi.org/10.1007/s11434-015-0922-9.

(34) Liu, J.; Falcoz, Q.; Gauthier, D.; Flamant, G.; Zheng, C. Z. Volatilization Behavior of Cd and Zn Based on Continuous Emission Measurement of Flue Gas from Laboratory-Scale Coal Combustion. *Chemosphere* **2010**, *80* (3), 241–247. https://doi.org/10.1016/j.chemosphere.2010.04.028.

(35) Dilks, R. T.; Monette, F.; Glaus, M. The Major Parameters on Biomass Pyrolysis for Hyperaccumulative Plants - A Review. *Chemosphere* **2016**, *146*, 385–395. https://doi.org/10.1016/j.chemosphere.2015.12.062.

(36) Lei, M.; Dong, Z.; Jiang, Y.; Longhurst, P.; Wan, X.; Zhou, G. Reaction Mechanism of Arsenic Capture by a Calcium-Based Sorbent during the Combustion of Arsenic-Contaminated Biomass: A Pilot-Scale Experience. *Front. Environ. Sci. Eng.* **2019**, *13* (2). https://doi.org/10.1007/s11783-019-1110-y.

(37) Mayer, Z. A.; Apfelbacher, A.; Hornung, A. A Comparative Study on the Pyrolysis of Metal- and Ash-Enriched Wood and the Combustion Properties of the Gained Char. *J. Anal. Appl. Pyrolysis* **2012**, *96*, 196–202. https://doi.org/10.1016/j.jaap.2012.04.007.

(38) Yan, Y.; Clough, P. T.; Anthony, E. J. Investigation of the Apparent Kinetics of Air and Oxy-Fuel Biomass Combustion in a Spout Fluidised-Bed Reactor. *Chem. Eng. Res. Des.* **2020**. https://doi.org/10.1016/j.cherd.2019.10.043.

(39) Zha, J.; Huang, Y.; Xia, W.; Xia, Z.; Liu, C.; Dong, L.; Liu, L. Effect of Mineral Reaction between Calcium and Aluminosilicate on Heavy Metal Behavior during Sludge Incineration. *Fuel* **2018**, *229* (April), 241–247. https://doi.org/10.1016/j.fuel.2018.05.015.

(40) LI, X.; ZHANG, W.; LU, J.; WANG, L. Calcium Oxalate Biomineralization in Plants. *Chinese Sci. Bull. (Chinese Version)* **2012**, *57* (26), 2443. https://doi.org/10.1360/972012-603.

(41) Cao, W.; Li, J.; Lin, L.; Zhang, X. Release of Potassium in Association with Structural Evolution during Biomass Combustion. *Fuel* **2021**, *287* (November 2020), 119524. https://doi.org/10.1016/j.fuel.2020.119524.

(42) Deng, L.; Jin, X.; Long, J.; Che, D. Ash Deposition Behaviors during Combustion of Raw and Water Washed Biomass Fuels. *J. Energy Inst.* **2019**, *92* (4), 959–970.

https://doi.org/10.1016/j.joei.2018.07.009.

(43) Wang, X.; Zhai, M.; Guo, H.; Panahi, A.; Dong, P.; Levendis, Y. A. High-Temperature Pyrolysis of Biomass Pellets: The Effect of Ash Melting on the Structure of the Char Residue. *Fuel* **2021**, *285* (August 2020), 119084. https://doi.org/10.1016/j.fuel.2020.119084.

(44) Raeva, A. A.; Klykov, O. V.; Kozliak, E. I.; Pierce, D. T.; Seames, W. S. In Situ Evaluation of Inorganic Matrix Effects on the Partitioning of Three Trace Elements (As, Sb, Se) at the Outset of Coal Combustion. *Energy and Fuels* **2011**, *25* (10), 4290–4298. https://doi.org/10.1021/ef200879j.

(45) Niu, Y.; Tan, H.; Hui, S. Ash-Related Issues during Biomass Combustion: Alkali-Induced Slagging, Silicate Melt-Induced Slagging (Ash Fusion), Agglomeration, Corrosion, Ash Utilization, and Related Countermeasures. *Prog. Energy Combust. Sci.* **2016**, *52*, 1–61. https://doi.org/10.1016/j.pecs.2015.09.003.

Graphical Abstract

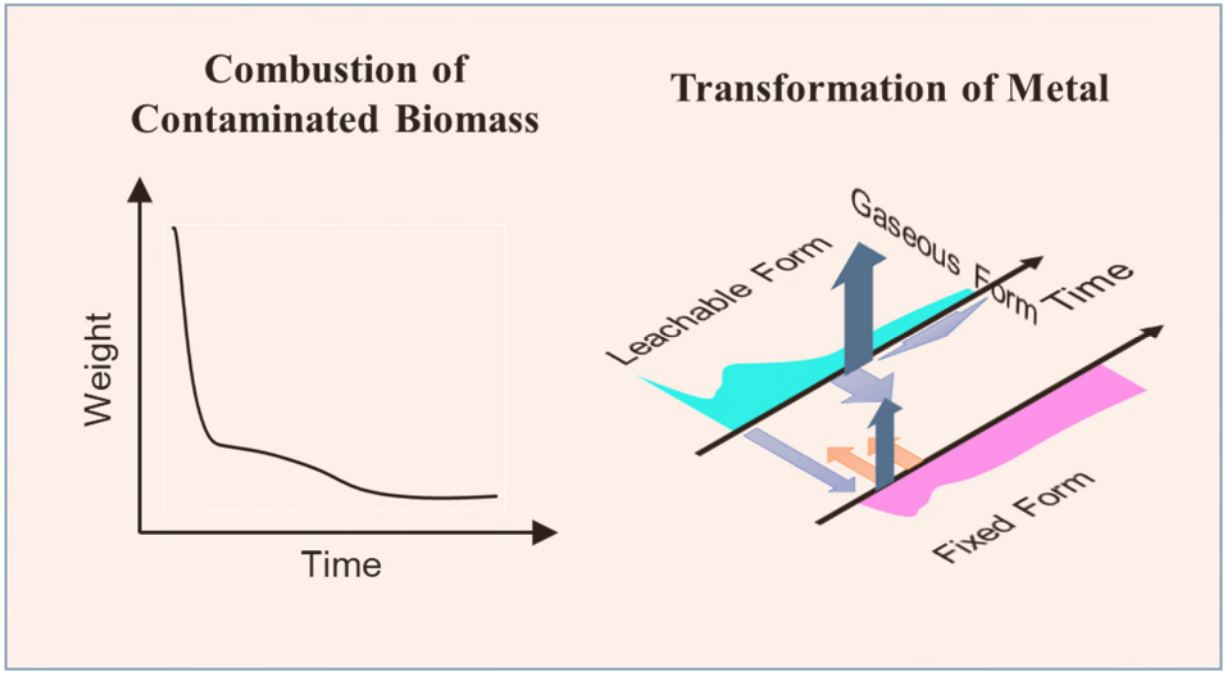

Synopsis

Metal transformations in the burning solid matter were revealed during the combustion process of a kind of hyper-accumulator biomass.